Analytical Study on the Wave Scattering by Canonical Two-Dimensional Obstacles

Takashi Nagasaka
Electrical, Electronic, and Communication Engineering Course
Graduated School of Science of Engineering

1. Introduction

The analysis of the scattering and diffraction by canonical obstacles is an important subject in electromagnetic theory and radar cross section (RCS) studies. Various analytical and numerical methods have been developed thus far and the scattering have been investigated for a number of two- and three-dimensional obstacles. Among a number of analysis methods, the Wiener-Hopf technique [1] is known as a rigorous, function-theoretic approach for electromagnetic wave problems related to canonical geometries.

The aims of this dissertation are to analyze the diffraction by two-dimensional obstacles having various physical parameters applying the Wiener-Hopf technique. In particular, we shall consider a material strip with various physical parameters involving the obstacles with arbitrary permittivity and permeability, and analyze the plane wave diffraction by a thin material via use of the Wiener-Hopf technique.

In past related research, Volakis [2] analyzed the H-polarized plane wave diffraction by a thin material strip using the dual integral equation approach and the extended spectral ray method together with approximate boundary conditions [3]. In [2], Volakis first solved rigorously the diffraction problem involving a single material half-plane, and subsequently obtained a high-frequency solution to the original strip problem by superposing the singly diffracted fields from the two independent half-planes and the doubly/triply diffracted fields from the edges of the two half-planes. Therefore his analysis is not rigorous in the sense of boundary value problems, and may not be applicable unless the strip width is relatively large compared with the wavelength. This problem has been solved more recently by Shapoval *et al*. [4] by using the generalized boundary conditions and the singular integral equation.

In following sections, we shall consider the same Volakis's problem [2], and analyze the plane wave diffraction by a thin material strip for both E and H polarizations using Wiener-Hopf technique and approximate boundary conditions [3]. Analytical details are presented only for the E-polarized case, but numerical results will be shown for both E and H polarizations. Introducing the Fourier transform for the unknown scattered field and applying boundary conditions [3] in the transform domain, the problem is formulated in terms of the Wiener-Hopf equations, which are solved exactly via the factorization and decomposition procedure. However, the solution is formal in the sense that branch-cut integrals with unknown integrands are involved. By using a rigorous asymptotic method, together with a special function introduced by authors [5], we have derived a high-frequency solution for Wiener-Hopf equations, which is described in terms of an infinite asymptotic series. Taking the Fourier inverse of the solution in the transform domain and applying the saddle point method, the scattered far field in the real space is derived. Numerical examples of the RCS are shown for various physical parameters, and scattering characteristics of the strip are discussed in detail. The results of this paper are published in Nagasaka and Kobayashi [5, 6].

The time factor is assumed to be $e^{-i\omega t}$ and suppressed throughout this dissertation.

2. Formulation of the Problem

We consider the diffraction of an E-polarized plane wave by a thin material strip as shown in Figure 1, where the relative permittivity and permeability of the strip are denoted by ε_r and μ_r, respectively. Let the total electric field $\phi^t(x,z)[\equiv E_y^t(x,z)]$ be

$$\phi^t(x,z) = \phi^i(x,z) + \phi(x,z), \tag{1}$$

where $\phi^i(x,z)$ is the incident field given by

$$\phi^i(x,z) = e^{-ik(x\sin\theta_0 + z\cos\theta_0)}, \quad 0 < \theta_0 < \pi/2 \tag{2}$$

with $k[=\omega(\varepsilon_0\mu_0)^{1/2}]$ being the free-space wavenumber. The term $\phi(x,z)$ is the unknown scattered field and satisfies the two-dimensional Helmholtz equation.

If the strip thickness b is small compared with the wavelength, the material strip is approximately replaced by a strip of zero thickness satisfying the approximate boundary conditions [3]. On the strip surface, the total electromagnetic fields satisfy the approximate boundary conditions as given by

$$\left[\frac{1}{R_e} + \frac{1}{\tilde{R}_m}\left(1 + \frac{1}{k^2}\frac{\partial^2}{\partial x^2}\right)\right][E_y^t(+0,z) + E_y^t(-0,z)] = -2[H_z^t(+0,z) - H_z^t(-0,z)], \tag{3}$$

$$[H_z^t(+0,z) + H_z^t(-0,z)] = -2R_m[E_y^t(+0,z) - E_y^t(-0,z)], \tag{4}$$

where

$$\left.\begin{aligned} &R_e = iZ_0/[kb(\varepsilon_r - 1)],\ R_m = iY_0/[kb(\mu_r - 1)], \\ &\tilde{R}_m = iZ_0\mu_r/[kb(\mu_r - 1)] \end{aligned}\right\} \tag{5}$$

with Z_0 and Y_0 being the intrinsic impedance and admittance of free space, respectively.

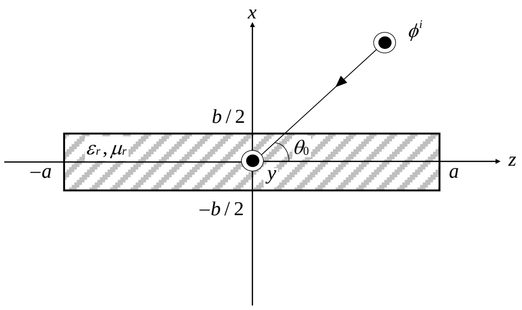

Figure 1. Geometry of the problem.

In the following, we shall assume that the medium is slightly lossy as in $k = k_1 + ik_2$ with $0 < k_2 \ll k_1$.

Let us define the Fourier transform of the scattered field $\phi(x,z)$ with respect to z as

$$\Phi(x,\alpha) = (2\pi)^{-1/2} \int_{-\infty}^{\infty} \phi(x,z) e^{i\alpha z} dz, \qquad (6)$$

where $\alpha = \sigma + i\tau$. Then we see with the aid of the radiation condition that $\Phi(x,\alpha)$ is regular in the strip $|\tau| < k_2 \cos\theta_0$ of the complex α-plane. Introducing the Fourier integrals as

$$\Phi_{\pm}(x,\alpha) = \pm(2\pi)^{-1/2} \int_{\pm a}^{\pm\infty} \phi(x,z) e^{i\alpha(z \mp a)} dz, \qquad (7)$$

it is found that $\Phi_{\pm}(x,\alpha)$ are regular in $\tau \gtrless \mp k_2 \cos\theta_0$. Taking the Fourier transform of the Helmholtz equation and solving the resultant equation, we find that

$$\Phi(x,\alpha) = \hat{\Phi}(\alpha) e^{-\gamma|x|}, \qquad (8)$$

where $\gamma = (\alpha^2 - k^2)^{1/2}$ with $\mathrm{Re}\,\gamma > 0$, and

$$\hat{\Phi}(\alpha) = -ikZ_0[e^{-i\alpha a}U_-(\alpha) + e^{i\alpha a}U_{(+)}(\alpha)]/[2\gamma M(\alpha)]$$
$$\mp [e^{-i\alpha a}V_-(\alpha) + e^{i\alpha a}V_{(+)}(\alpha)]/K(\alpha), \quad x \gtrless 0 \qquad (9)$$

with

$$K(\alpha) = \gamma - 2ikZ_0R_m, \qquad (10)$$

$$M(\alpha) = 1 - \frac{ikZ_0}{2\gamma}\left[\frac{1}{R_e} + \frac{1}{\tilde{R}_m}\left(1 + \frac{\gamma^2}{k^2}\right)\right], \qquad (11)$$

$$V_{\substack{(+)\\-}}(\alpha) = \Phi'_{\pm}(\alpha) \mp \frac{B_{1,2}}{\alpha - k\cos\theta_0}, \qquad (12)$$

$$U_{\substack{(+)\\-}}(\alpha) = \tilde{\Phi}_{\pm}(\alpha) \mp \frac{A_{1,2}}{\alpha - k\cos\theta_0}, \qquad (13)$$

$$\Phi'_{\pm}(\alpha) = \frac{d\Phi_{\pm}(0,\alpha)}{dx}, \qquad (14)$$

$$\tilde{\Phi}_{\pm}(\alpha) = \left(\frac{1}{R_e} + \frac{1}{\tilde{R}_m}\right)\Phi_{\pm}(0,\alpha) + \frac{1}{\tilde{R}_m k^2}\frac{d^2\Phi_{\pm}(0,\alpha)}{dx^2}, \qquad (15)$$

$$B_{1,2} = -(2\pi)^{-1/2} k \sin\theta_0 e^{\mp ika\cos\theta_0}, \qquad (16)$$

$$A_{1,2} = -(2\pi)^{-1/2} i\left(\frac{1}{R_e} + \frac{\cos^2\theta_0}{\tilde{R}_m}\right)e^{\mp ika\cos\theta_0}. \qquad (17)$$

Equation (8) is the scattered field representation in the Fourier transform domain. Using the boundary conditions, we obtain from (9) that

$$-K(\alpha)J_m(\alpha) = 2[e^{-i\alpha a}V_-(\alpha) + e^{i\alpha a}V_{(+)}(\alpha)], \qquad (18)$$

$$M(\alpha)J_e(\alpha) = e^{-i\alpha a}U_-(\alpha) + e^{i\alpha a}U_{(+)}(\alpha), \qquad (19)$$

where $J_e(\alpha)$ and $J_m(\alpha)$ denote the Fourier transforms of the unknown electric and magnetic surface currents on the strip, respectively, and are entire functions. Equations (18) and (19) are the Wiener-Hopf equations satisfied by the unknown spectral functions.

3. Exact Solution

The kernel functions $M(\alpha)$ and $K(\alpha)$ defined by (10) and (11) can be factorized as

$$K(\alpha) = K_+(\alpha)K_-(\alpha) = K_+(\alpha)K_+(-\alpha), \qquad (20)$$

$$M(\alpha) = M_+(\alpha)M_-(\alpha) = M_+(\alpha)M_+(-\alpha), \qquad (21)$$

where

$$K_{\pm}(\alpha) = (2kZ_0R_m)^{1/2} e^{-i\pi/4} N_{3\pm}(\alpha), \qquad (22)$$

$$M_{\pm}(\alpha) = \left[\frac{kZ_0}{2}\left(\frac{1}{R_e} + \frac{1}{\tilde{R}_m}\right)\right]^{1/2} \frac{N_{1\pm}(\alpha)N_{2\pm}(\alpha)}{(k \pm \alpha)^{1/2}} \qquad (23)$$

with

$$N_{n\pm}(\alpha) = (1 + \delta_n^{-1})^{1/2}$$
$$\cdot \exp\left\{-\frac{\delta_n}{\pi}\int_{\pi/2}^{\arccos(\pm\alpha/k)} \frac{t\cos t}{\sin^2 t - \delta_n^2} dt\right.$$
$$+ \frac{1}{4}\ln\left[1 + \frac{\alpha^2}{k^2(\delta_n^2 - 1)}\right] \pm \ln[\delta_n + (\delta_n^2 - 1)^{1/2}]$$
$$\left.\cdot \frac{i}{2\pi}\ln\left[\frac{ik(\delta_n^2 - 1)^{1/2} + \alpha}{ik(\delta_n^2 - 1)^{1/2} - \alpha}\right]\right\}, \quad n = 1,2,3, \qquad (24)$$

$$\left.\begin{aligned} \delta_{1,2} &= -\frac{\tilde{R}_m}{Z_0}\left\{1 \pm \left[1 + \frac{Z_0^2}{\tilde{R}_m}\left(\frac{1}{R_e} + \frac{1}{\tilde{R}_m}\right)\right]^{1/2}\right\}, \\ \delta_3 &= 2Z_0R_m. \end{aligned}\right\} \qquad (25)$$

We multiply both sides of (18) by $e^{\pm i\alpha a}/K_{\mp}(\alpha)$ and apply the decomposition procedure with the aid of the edge condition. This leads to

$$V_{(+)}^{s,d}(\alpha) = K_+(\alpha)\left[-\frac{B_1}{K_+(k\cos\theta_0)(\alpha - k\cos\theta_0)}\right.$$
$$\left.\mp \frac{B_2}{K_-(k\cos\theta_0)(\alpha + k\cos\theta_0)} \pm v_{s,d}(\alpha)\right], \qquad (26)$$

where

$$v_{s,d}(\alpha) = \frac{1}{\pi i}\int_k^{k+i\infty} \frac{e^{2i\beta a}(\beta - k)^{1/2}}{\beta + \alpha} V_{(+)}^{s,d}(\beta) T_+(\beta) d\beta, \qquad (27)$$

$$V_{(+)}^{s,d}(\alpha) = V_{(+)}(\alpha) \pm V_-(-\alpha) \qquad (28)$$

with

$$T_+(\beta) = \frac{(\beta + k)^{1/2} K_+(\beta)}{\beta^2 - k^2 + 4k^2Z_0^2R_m^2}. \qquad (29)$$

Equation (26) is the exact solution to the Wiener-Hopf equation (18), but it is formal since the branch-cut integrals with the unknown integrands $v_{s,d}(\alpha)$ are involved. Equation (19) can be solved in a similar manner.

4. High-Frequency Asymptotic Solution

In order to eliminate the singularities of $V^{s,d}_{(+)}(\alpha)$ in (26) at $\alpha = k\cos\theta_0$, we introduce the functions

$$\Phi'^{s,d}_{+}(\alpha) = \Phi'_{+}(\alpha) \pm \Phi'_{-}(-\alpha). \tag{30}$$

Applying the asymptotic method [5] developed by the second-named author, we can obtain a high-frequency asymptotic expansion of (26) with the result that

$$\Phi'^{s,d}_{+}(\alpha) \sim K_{+}(\alpha) \cdot \left[\chi_{vs,vd}(\alpha) + C_{s,d} \sum_{n=0}^{N} f_n^{vs,vd} \xi^t_{0n}(\alpha) \right] \tag{31}$$

for $ka \to \infty$, where N denotes the truncation number of the infinite asymptotic series. In (31), several quantities are defined by

$$\chi_{vs,vd}(\alpha) = B_1[Q_1(\alpha) \pm \eta_{t2}(\alpha)] + B_2[\eta_{t1}(\alpha) \pm Q_2(\alpha)], \tag{32}$$

$$C_{s,d} = \pm 1, \tag{33}$$

$$f_n^{vs,vd} = \frac{1}{n!} \frac{d^n \Phi'^{s,d}_{+}(\alpha)}{d\alpha^n}\bigg|_{\alpha=k}, \tag{34}$$

$$\xi^t_{pn}(\alpha) = \frac{e^{2ika}}{\pi}(-1)^p p! \frac{i^{n-p-1/2}}{(2a)^{n-p+1/2}} \cdot \Gamma^t_{p+1}[3/2+n, -2i(\alpha+k)a], \tag{35}$$

where

$$\eta_{t1,t2}(\alpha) = \frac{\xi^t_{00}(\alpha) - \xi^t_{00}(\pm k\cos\theta_0)}{\alpha \mp k\cos\theta_0}, \tag{36}$$

$$Q_{1,2}(\alpha) = \frac{1}{\alpha \mp k\cos\theta_0}\left[\frac{1}{K_{+}(\alpha)} - \frac{1}{K_{\pm}(k\cos\theta_0)}\right], \tag{37}$$

$$\Gamma^t_m(u,w) = \int_0^\infty \frac{t^{u-1}e^{-t}}{(t+w)^m} T_{+}[k + it/(2a)]dt. \tag{38}$$

Carrying out some manipulations, we can show the unknowns $f_n^{vs,vd}$ in (31) are determined by solving the matrix equation

$$f_m^{vs,vd} - C_{s,d}\sum_{n=0}^{N} A^v_{mn} f_n^{vs,vd} \sim B_m^{vs,vd} \tag{39}$$

for $m = 0,1,2,\cdots,N$, where

$$A^v_{mn} = \sum_{p=0}^{m} \frac{K_{+}^{(m-p)}(k)\xi^t_{pn}(k)}{p!(m-p)!}, \tag{40}$$

$$B_m^{vs,vd} = \sum_{p=0}^{m} \frac{K_{+}^{(m-p)}(k)\chi^{(p)}_{vs,vd}(k)}{p!(m-p)!} \tag{41}$$

with

$$K_{+}^{(m-p)}(k) = \frac{d^{m-p}K_{+}(\alpha)}{d\alpha^{m-p}}\bigg|_{\alpha=k}, \tag{42}$$

$$\chi^{(p)}_{vs,vd}(k) = \frac{d^p \chi_{vs,vd}(\alpha)}{d\alpha^p}\bigg|_{\alpha=k}. \tag{43}$$

Making use of the above results, we finally arrive at an explicit asymptotic solution to the Wiener-Hopf equation (18) with the result that

$$V_{(\overset{+}{-})}(\alpha) \sim K_{\pm}(\alpha)\left[\mp \frac{B_{1,2}}{K_{\pm}(k\cos\theta_0)(\alpha - k\cos\theta_0)} + B_{2,1}\eta_{t1,t2}(\pm\alpha) + \frac{1}{2}\sum_{n=0}^{N}(f_n^{vs} \mp f_n^{vd})\xi^t_{0n}(\pm\alpha)\right] \tag{44}$$

as $ka \to \infty$. A similar procedure may also be applied to (19) for a high-frequency solution, but the details will not be discussed here.

5. Scattered Far Field and Numerical Results

The scattered field in the real space is obtained by taking the inverse Fourier transform of (9) with the result that

$$\phi(\rho,\theta) \sim \hat{\Phi}(-k\cos\theta)k\sin|\theta|(k\rho)^{-1/2}e^{i(k\rho-\pi/4)} \tag{45}$$

as $k\rho \to \infty$. Equation (45) is uniformly valid for arbitrary incidence and observation angles.

We shall now present numerical results on the RCS for both E and H polarizations, and discuss the far field scattering characteristics of the strip in detail. The normalized RCS per unit length is defined by

$$\sigma/\lambda = \lim_{\rho\to\infty}\left(k\rho|\phi/\phi^i|^2\right) \tag{46}$$

with λ being the free-space wavelength. In computing (46), we have used the high-frequency asymptotic expressions as given by (44) for $V_{(\overset{+}{-})}(\alpha)$, where the truncation number N for the asymptotic series is contained. Let $\sigma^{(N)}$ and $\sigma^{(N+1)}$ be the RCS with the truncation numbers being N and $N+1$, respectively. In numerical computation, we have employed the convergence criteria $|\sigma^{(N+1)} - \sigma^{(N)}| < 10^{-3}$ in order to determine the desired truncation number N. By careful numerical investigation, we have verified that the choice of $N = 3$ satisfies the aforementioned convergence criteria and hence provides sufficiently accurate solutions.

Figure 2 shows the monostatic RCS as a function of incidence angle θ_0, where the strip width is $2a = 10\lambda$, the strip thickness is $b = 0.01\lambda$, and the truncation number of the infinite asymptotic series (44) is $N = 3$. As an example of existing lossy materials, we have chosen the ferrite [7] with $\varepsilon_r = 12.0 + i0$ and $\mu_r = 1.4 + i4.5$ in numerical computation. Comparing the RCS characteristics for E polarization with those for H polarization, we find that the RCS level for H polarization is lower than that for E polarization over the whole range of the incidence angle θ_0.

Figure 3 shows the monostatic RCS as a function of incidence angle θ_0 for H polarization, where the strip width is $2a = 1.7\lambda$, the strip thickness is $b = 0.01\lambda$, and the material parameters are $\varepsilon_r = 7.4 + i1.11$, $\mu_r = 1.4 + i0.672$. In the figure, we have also added the

Volakis's results [2]. It is seen from the figure that our results agree with Volakis's results [2].

Figure 4 shows the monostatic RCS as a function of incidence angle θ_0 for E polarization and its comparison with Shapoval's results [8]. The strip dimension is $2a = 5\lambda$, $b = 0.01\lambda$, the material parameters are $\varepsilon_r = 3.4 + i10, \mu_r = 1$, and $N = 3$. Wee see from the figure that our results agree quite well with Shapoval's results [8].

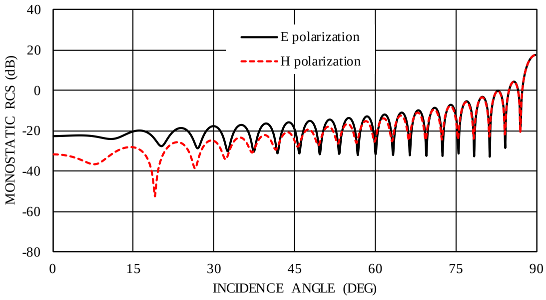

Figure 2. Monostatic RCS $\sigma^{(N)} / \lambda$ versus incidence angle θ_0 for $2a = 10\lambda$, $b = 0.01\lambda$, $\varepsilon_r = 12.0 + i0$, $\mu_r = 1.4 + i4.5$, $N = 3$.

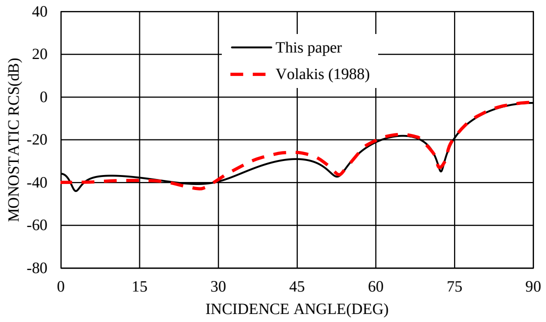

Figure 3. Monostatic RCS $\sigma^{(N)} / \lambda$ versus incidence angle θ_0 for H polarization, $\varepsilon_r = 7.4 + i1.11$, $\mu_r = 1.4 + i0.672$, $2a = 1.7\lambda, b = 0.01\lambda$, $N = 3$, and its comparison with Volakis [2].

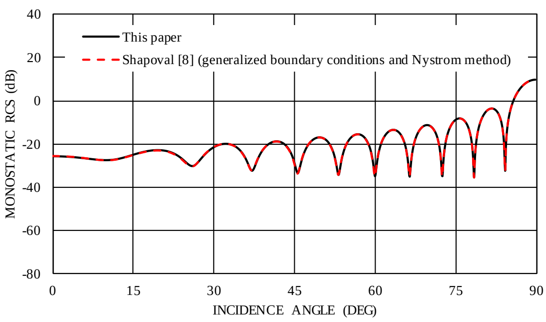

Figure 4. Monostatic RCS $\sigma^{(N)} / \lambda$ versus incidence angle θ_0 for E polarization, $\varepsilon_r = 3.4 + i10, \mu_r = 1$, $2a = 5\lambda$, $b = 0.01\lambda, N = 3$, and its comparison with Shapoval [8].

6. Conclusions

In this paper, we have solved the plane wave diffraction by a thin material strip for both E and H polarizations using the Wiener-Hopf technique together with approximate boundary conditions [3]. Employing a rigorous asymptotic method, a high-frequency solution for large strip width has been obtained. Illustrative numerical examples on the RCS are presented, and the far field scattering characteristics of the strip have been discussed in detail. Some comparisons with the other existing method have also been provided.

7. Acknowledgement

The authors would like to thank Dr. Olga V. Shapoval for providing various numerical results based on generalized boundary conditions and the singular integral equation.

References

1. B. Noble, *Methods Based on the Wiener-Hopf Technique for the Solution of Partial Differential Equations*, London, Pergamon, 1958.
2. J. L. Volakis, "High-frequency scattering by a thin material half plane and strip," *Radio Science*, **23**, 3, 1988, pp.450-462.
3. T. B. A. Senior and J. L. Volakis, *Approximate Boundary Conditions in Electromagnetics*, IEE, London, 1995.
4. O. V. Shapoval, R. Sauleau, and A. I. Nosich, "Scattering and absorption of waves by flat material strips analyzed using generalized boundary conditions and Nystrom-type algorithm," *IEEE Transactions on Antennas and Propagation*, **59**, 9, September 2011, pp.3339–3346.
5. T. Nagasaka and K. Kobayashi, "Wiener-Hopf analysis of the plane wave diffraction by a thin material strip," *IEICE Transactions on Electronics*, **E100-C**, 1, January 2017, pp.11-19.
6. T. Nagasaka and K. Kobayashi, "Wiener-Hopf analysis of the plane wave diffraction by a thin material strip: the case of E polarization," *IEICE Transactions on Electronics*, **E101-C**, 1, January 2018, pp.12-19.
7. T. Komoni, F. Yasuda and K. Saito, "Development of the demountable damped cavity," *Proceedings of 15th International Conference on RF Superconductivity*, July 2011, pp.172-176.
8. O. V. Shapoval, private communication, September 2016.